Application Note:
Cancer Research

Nabsys

High-Resolution Detection of Cancer-Associated SVs Using EGM

Mapping *TP53* Deletions and *PML::RARA* Fusions with the OhmX™ Platform

Abstract

Deletions in the tumor protein p53 (*TP53*) gene—a critical tumor suppressor—are associated with adverse outcomes across a variety of cancers, including hematologic malignancies. Likewise, fusion events involving promyelocytic leukemia (*PML*) and retinoic acid receptor alpha (*RARA*) genes, particularly the canonical *PML::RARA* fusion, are hallmark drivers of acute promyelocytic leukemia (APL) and have direct implications for diagnosis and treatment decisions. Detecting such structural variants (SVs) with precision remains a significant clinical challenge. Short-read sequencing (SRS) often misses large SVs due to read-length constraints, while long-read sequencing (LRS) and traditional cytogenetic techniques struggle to balance resolution, throughput, and cost.

This application note demonstrates the utility of the Nabsys OhmX™ Platform, powered by electronic genome mapping (EGM), to detect clinically relevant *TP53* deletions and *PML::RARA* translocations in commercially available leukemia and cancer cell lines. EGM's high tag density in the gene regions and resolution enabled accurate identification of *TP53* deletions ranging from 3.8 kb to 87 kb and precise mapping of reciprocal *PML::RARA* fusion breakpoints. The breakpoints were confirmed using Nabsys SV-Verify™ software and were concordant with orthogonal data from microarrays and literature. Together, these results support the potential of EGM as a valuable tool for high-resolution SV detection in clinical oncology research, offering genome-wide coverage for key pathogenic events.

Key Features and Benefits

- **High-Resolution Mapping:** Enables detection of challenging SVs with kilobase-level resolution
- **Comprehensive Analysis:** Combines genome-wide discovery and targeted SV confirmation
- **Cost-Effective and Scalable:** Achieves high-resolution insights affordably and efficiently
- **High Tag Density:** Higher tag density across critical regions (11 tags in *TP53*, plus dense coverage in *PML* and *RARA* genes) vs. limited optical labeling, enabling detection of challenging SVs

Introduction

In the development and progression of leukemia, SVs such as deletions, translocations, and gene fusions, play essential roles and are often used as biomarkers for diagnosis, prognosis, and treatment selection. Two well-characterized genomic alterations associated with leukemia are deletions in the *TP53* gene and the fusion of the *PML* and *RARA* genes.[1–3]

Variants in *TP53*, a tumor suppressor gene, are especially prevalent in aggressive adult and pediatric hematologic malignancies.[4] *TP53* mutations are found in approximately 5% to 10% of patients with de novo AML, and are more frequently observed in elderly patients and those with therapy-related AML.[5] Disruption of *TP53* function—whether via mutation or deletion—compromises DNA damage response, cell-cycle control, and programmed cell death, contributing to genomic instability, chemotherapy resistance, and poor clinical outcomes.[6,7]

A hallmark fusion event in APL is the *PML::RARA* translocation, resulting from the reciprocal t(15;17)(q24;q21) chromosomal rearrangement.[3] This fusion protein links *PML* to the DNA-binding region of *RARA* and exerts a dominant-negative effect that blocks myeloid differentiation at the promyelocytic stage.[8,9] In APL, prompt detection of the *PML::RARA* fusion is essential due to the high risk of coagulopathy and early mortality if left untreated.[3] The effectiveness of all-trans retinoic acid (ATRA) therapy is directly attributable to its ability to bind and degrade the fusion protein. ATRA therapy has revolutionized APL treatment, yielding remission rates beyond 90%.[10]

Despite their clinical importance, these leukemia-associated SVs can be difficult to detect with existing technologies. SRS lacks the genomic context and resolution to accurately identify large deletions or complex rearrangements, while LRS

offers improvements but can be cost-prohibitive. Standard cytogenetic methods like karyotyping, fluorescence in situ hybridization (FISH), and chromosomal microarray analysis (CMA) are widely used in clinical settings but often fail to resolve smaller or cryptic variants.[11,12] Optical genome mapping (OGM) has addressed some of these limitations, but its resolution is restricted by the diffraction limits of optical imaging and a relatively low label density in the regions analyzed here (*TP53*, *PML*, and *RARA* gene regions).[13]

In contrast, EGM offers a sequence-specific, electronic detection approach that is capable of both whole-genome SV discovery and targeted, hypothesis-driven variant confirmation at sub-kb resolution.[14] EGM is well-suited to resolving the spectrum of clinically-relevant variants involved in leukemogenesis, with precise fusion breakpoint mapping and high tag density in the *TP53*, *PML*, and *RARA* loci, though the density varies from gene to gene. The approval of a Current Procedural Terminology (CPT) code for OGM in January 2025 further underscores the growing clinical value of high-resolution SV technologies, highlighting a path toward the adoption of complementary tools like EGM in diagnostic settings.

In this study, we applied EGM using the OhmX Platform to analyze two leukemia-derived cell lines (HL-60 and NB-4) and a non-small cell lung cancer (NSCLC) cell line (H1299, known for its lack of p53 expression) to demonstrate the detection of homozygous *TP53* deletions ranging from approximately 3.8 kb to 87 kb and canonical reciprocal *PML::RARA* translocations. The results establish EGM's potential and position the Nabsys OhmX Analyzer as a high-confidence platform for detecting clinically-relevant variants.

Methods

Sample Preparation

Three commercially available cancer cell lines, HL-60 (leukemia, HL-60; ATCC CCL-240), NCI-H1299 (NSCLC cancer, H1299; ATCC CRL-5803), and NB-4 (APL, NB-4; Cytion Catalog #300299), were purchased from ATCC and Cytion. A reference cell line, HG002, was obtained from the NIGMS Human Genetic Cell Repository at the Coriell Institute for Medical Research (NA24385). High molecular weight (HMW) DNA was extracted from each cell line using the Monarch® HMW DNA Extraction Kit for Cells & Blood (New England Biolabs®, Catalog #T3050) and the DNA Isolation for OhmX Sample Preparation Guide (Document #755-00017-001). The quantity and quality of the isolated DNA were evaluated using a NanoDrop™ spectrophotometer (Thermo Fisher Scientific®) and pulsed-field gel electrophoresis (PFGE).

After DNA isolation, each sample was nicked with BspQI and BssSI enzymes and labeled with modified nucleotides using the OhmX Simultaneous Nicking and Labeling Sample Preparation Kit (Part #900-00063-001) and the OhmX Sample Preparation Kit Guide (Document #755-00011-001). To enable electronic detection, the modified nucleotides at each site were tagged. The entire genome was then coated with RecA protein, which stiffens the DNA and further enhances detection.

Electronic Genome Mapping

Each sample was injected into an OhmX Analyzer equipped with an OhmX Detector. For each sample, the reagent and detector lot numbers were recorded to ensure traceability. Data was collected for each sample until sufficient coverage was reached.

Raw electronic signal data (TDD files) were generated by the OhmX Analyzer and securely archived in both the Human Chromosome Explorer™ (HCE) and internal servers. Remapped data were produced using the HDM Analysis Remap pipeline and also stored in HCE. For analysis, all data were uploaded to HCE, where initial quality control (QC) was performed. *De novo* assembly was initiated only if QC metrics were met.

Quality metrics assessed for data acceptance included: HCE estimated coverage ≥ approximately 150x (HL-60: 172x, H1299: 225x, NB-4: 294x, HG002: 145x), molecule N50 > 100 kb, and mean interval size between 4.1–4.54 kb (approximately 22–24 labels per 100 kb). Additional HCE assembly metrics were also evaluated, including a covered sites ratio > 85% and a map N50 > 1.1 Mb. All molecule statistics from HDM Analysis and instrument runs were reviewed within HCE to verify that minimum thresholds were met before structural variant analysis.

These same high-quality datasets were used in SV-Verify for hypothesis-based SV confirmation. Assembly data generated by HCE were retained within the HCE system for further downstream analysis.

Data Analysis and SV Calling

Initial read alignment was conducted using the HDM Analysis Remap pipeline, which mapped labeled molecules to the human reference genome. Molecule files were then uploaded to the HCE cloud platform (v. 20250401) for *de novo* map assembly and SV discovery against the hg38 reference genome. Maps and SV calls were visualized in the HCE interface using a BED file containing exon coordinates to aid interpretation of breakpoints.

SVs were characterized by breakpoint location (for deletions), fusion breakpoints (for translocations), size, zygosity, and SV

frequency. All SVs were visually validated using supporting contig stacks and molecule reads.

Raw data were also uploaded to SV-Verify, which tested each variant hypothesis by comparing alignment patterns against both wild-type (WT) and SV-specific constructs. SV-Verify sample run results were interpreted using established SV frequency thresholds to confirm variant presence or absence.

SVs were curated and evaluated based on multiple criteria, including breakpoint precision, size, zygosity, SV frequency, and concordance with orthogonal data such as next-generation sequencing (NGS), CMA, FISH, and karyotyping.

Results and Discussion

Detection of *TP53* Deletions

The high tag density of EGM workflows in the *TP53* gene (11 tags) suggests that it should be feasible to detect *TP53* SVs with sub-genic resolution using the OhmX Platform (**Figure 1**).

Homozygous deletions in the *TP53* gene in two cell lines, HL-60 (leukemia) and H1299 (NSCLC), were successfully detected using EGM (**Figure 2**, **Table 1**). In the HL-60 cell line, a homozygous deletion of approximately 87 kb was identified. This deletion spanned the *TP53* locus and was supported

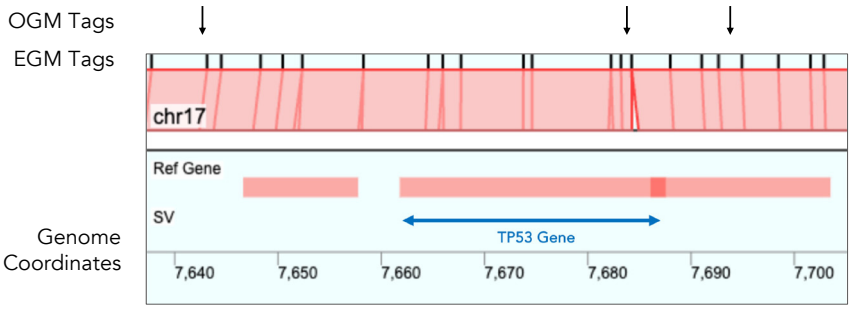

Figure 1: Comparison of label density between EGM and OGM in the *TP53* gene region. a) *TP53* gene region (hg38) visualized in HCE, with the gene represented as a blue arrow. EGM tags are represented by black vertical bars and OGM labels are represented as black arrows.

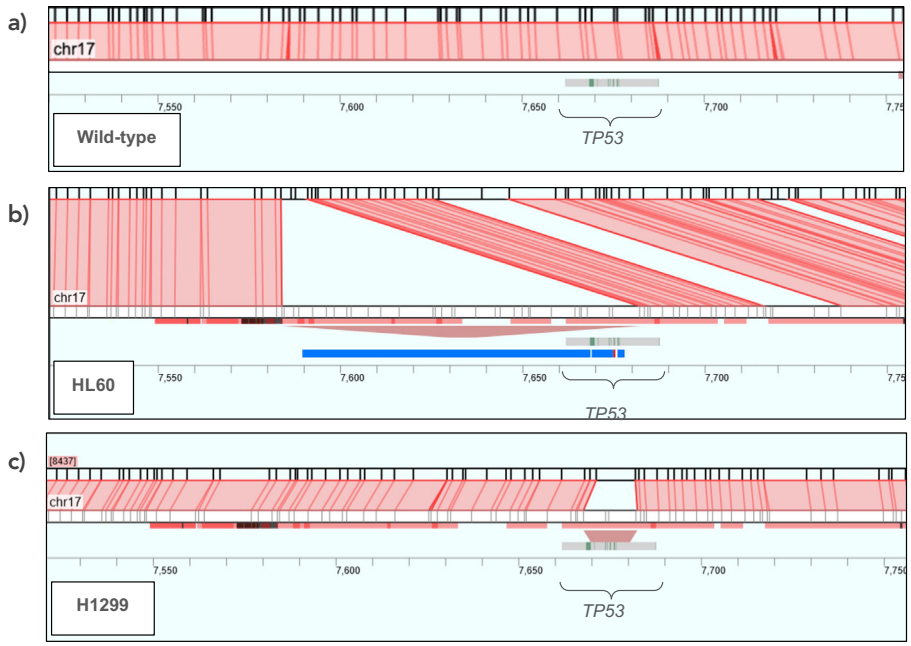

Figure 2: *TP53* deletions in healthy and cancer cell line samples visualized in HCE. *TP53* exon information is visualized using a custom BED file, with the gene represented as grey and red rectangles and exons shown in green. Deletions are represented as red trapexoids below the alignment. **a)** Negative control HG002 with WT *TP53* gene. **b)** Large, 87 kb *TP53* deletion in the HL-60 cell line. **c)** Small, 3.8 kb *TP53* deletion in the H1299 cell line.

Sample	Chr	Start	Length (bp)	Type	Zygosity
HL-60	17	7,583,898	90,663	Deletion	Homozygous
H1299	17	7,667,694	3,828	Deletion	Homozygous

Table 1: HCE summary statistics for *TP53* SV calls. *TP53* deletions were called in both the HL-60 and H1299 cell lines.

Sample	Chr	Start	Length (bp)	Type	Molecules Aligned to WT	Molecules Aligned to SV Hypothesis	SV Frequency
HL-60	17	7,589,540	87,389	Deletion	3	19	0.86
H1299	17	7,667,694	3,828	Deletion	25.5	34	0.57

Table 2: SV-Verify summary statistics for *TP53* SV calls. *TP53* deletions were confirmed in both the HL-60 and H1299 cell lines.

Chr	Start	End	Length (bp)
17	7,589,540	7,668,534	78,994
17	7,668,886	7,674,811	5,925
17	7,674,828	7,675,361	533
17	7,675,973	7,677,910	1,937
			87,389

Table 3: Chromosomal microarray data confirming copy number loss events *in the TP53* and upstream genomic region in the HL-60 cell line. The last row of the table shows the total length of all detected copy number loss events.

by contig alignment and a significant drop in molecule coverage across the deleted region. In the H1299 cell line, a small homozygous deletion of approximately 3.8 kb, also encompassing part of the *TP53* locus, was detected.

Hypothesis-based confirmation using SV-Verify showed strong support for the hypothesized SV in the HL-60 cell line—3 out of 19 molecules aligned to the SV hypothesis construct, with a calculated SV frequency of 0.86 (**Table 2**). These findings were corroborated by copy number microarray data indicating loss of the *TP53* region and upstream genomic sequence and results published by Wolf and Rotter (**Table 3**).[1] In the H1299 variant, SV-Verify analysis revealed 34 molecules aligning to the SV hypothesis and 25 aligning to the WT model, resulting in an SV frequency of 0.57 (**Table 2**).

The high tag density across the *TP53* region (11 tags) and sub-kb resolution enabled EGM to identify both large and small deletions with precise breakpoint mapping. These results highlight the OhmX Platform's ability to resolve variants below the resolution limit of optical methods, with accurate breakpoint precision in the sub-kb range.

Detection of *PML::RARA* Fusion Translocations

The high tag density of EGM workflows in the *PML* and *RARA* gene regions suggests that it should also be feasible to detect SVs in *PML* and *RARA* with high resolution using the OhmX Platform (**Figure 3**).

In the NB-4 APL cell line, reciprocal translocations between chromosomes 15 and 17 corresponding to the canonical *PML::RARA* fusion were identified using EGM (**Figure 4**). The first breakpoint was located at chr15:74,032,264–74,079,760 and joined to chr17:40,307,908–83,240,123, which resulted in the fusion of a small region of *PML* to *RARA* (**Table 4**). The reciprocal breakpoint occurred at chr17:40,348,576–40,723,935 and fused to chr15:74,034,747–101,977,640, which resulted in the fusion of a small region of *RARA* to *PML*.

These breakpoints were visualized and confirmed using contig-level alignments in HCE. EGM provided molecule-level resolution and showed full support for both fusion breakpoints. The reciprocal nature of the breakpoints is consistent with the classical t(15;17)(q24;q21) translocation seen in APL.

Hypothesis-based confirmation using SV-Verify showed strong support for the fusion—37 out of 98 molecules aligned to the SV hypothesis construct, with an SV frequency of 0.38 (**Table 5**).

The ability to resolve both breakpoints of a *PML::RARA* reciprocal fusion—along with supporting molecule evidence—demonstrates the utility of EGM for identifying balanced translocations.

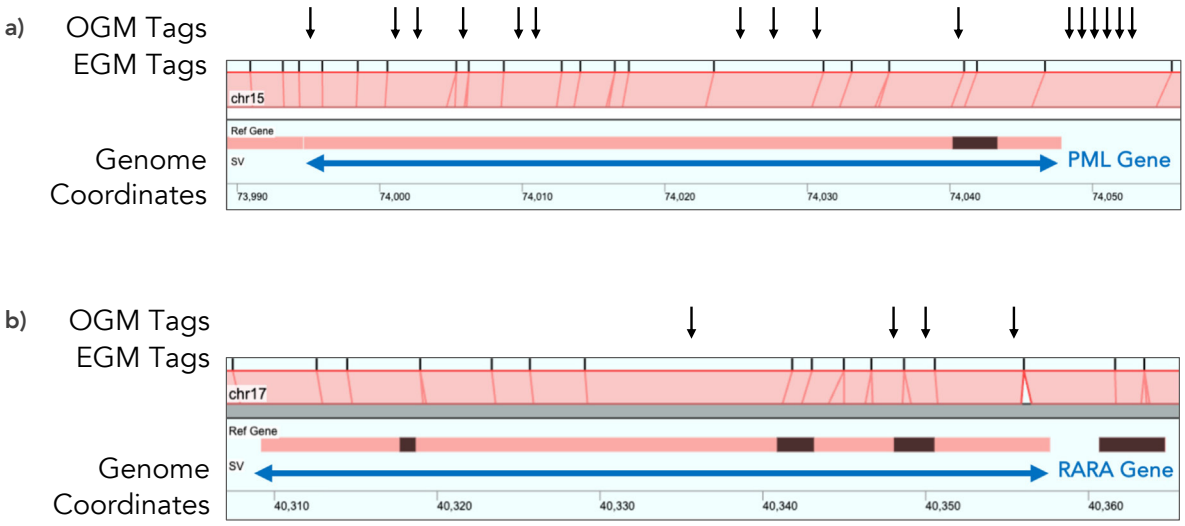

Figure 3: Comparison of label density between EGM and OGM at the *PML* and *RARA* genes. a) Genes regions are represented by blue arrows. EGM tags are represented by black vertical bars and OGM labels are represented as black arrows. **a.)** *PML* gene region (hg38) visualized in HCE. **b.)** *RARA* gene region (hg38) visualized in HCE.

Sample	Chr	Start	Length (bp)	Chr (To)	Start (To)	Length (To)	Type
NB-4	15	74,032,264	1,358	17	40,307,908	42,932,215	Transloc
NB-4	17	40,358,576	1,168	15	74,034,747	27,942,760	Transloc

Table 4: HCE summary statistics for *PML::RARA* SV calls. A balanced reciprocal *PML::RARA* translocation was called in the NB-4 cell line. Zygosity could not be determined using HCE.

Sample	Chr	Start	Chr (To)	Start (To)	Type	Molecules Aligned to WT	Molecules Aligned to SV Hypothesis	SV Frequency
NB-4	15	74,034,032	17	40,345,923	Breakpoint Fusion	60.5	37	0.3795

Table 5: SV-Verify summary statistics for *PML::RARA* SV calls. A *PML::RARA* breakpoint fusion was confirmed in the NB-4 cell line.

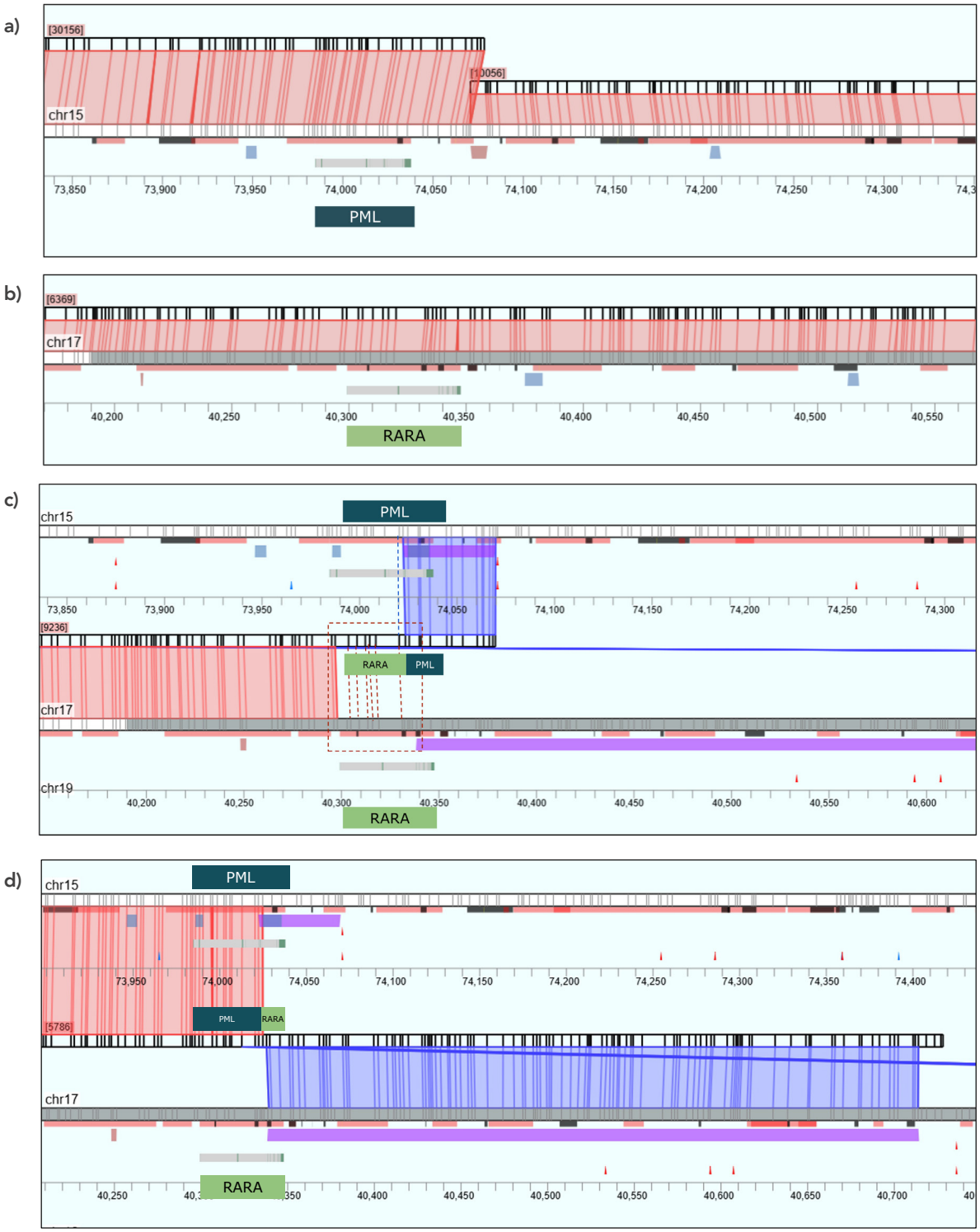

Figure 4: *PML::RARA* fusion in healthy and leukemia cell line samples visualized in HCE.
PML and *RARA* exon information is visualized using a custom BED file, with the gene represented as grey and red rectangles. Translocations are represented by purple rectangles. **a)** Negative control HG002 with WT *PML* gene. **b)** Negative control HG002 with WT *RARA* gene. **c)** First fusion breakpoint showing a small region of *PML* fused to *RARA* in the NB-4 cell line. **d)** Second fusion breakpoint showing a small region of *RARA* fused to *PML* in the NB-4 cell line.

Conclusion

This study demonstrates the analytical utility of EGM and the Nabsys OhmX Platform for high-resolution SV detection in leukemia and cancer models. EGM enabled high-confidence mapping of homozygous *TP53* deletions ranging from 3.8 kb to 87 kb and precise mapping of a reciprocal *PML::RARA* translocation using a dense, sequence-specific tagging strategy and electronic detection system with sub-kb resolution.

The OhmX Platform detected variants across a range of sizes with support from raw molecule data, contig-level assemblies in HCE, and independent hypothesis-based confirmation using SV-Verify. HCE employs a *de novo* assembly-based method to discover structural variants with high resolution, while SV-Verify uses an alignment-based approach to confirm hypotheses and provide additional metrics, such as SV frequency. Both tools independently deliver reliable and valuable insights, underscoring their utility in SV analysis.

The EGM-powered OhmX Platform demonstrated its value in translational cancer research with its ability to resolve different classes of genomic alterations that are difficult to detect. The OhmX Platform has the potential to be an indispensable tool in diagnosing APL and other leukemias, where timely detection of hallmark fusions like *PML::RARA* can influence treatment choice and clinical outcomes. Future efforts will focus on expanding the use of EGM on the OhmX Platform for more diverse clinical and research applications and integrating and enhancing analytical outputs.

The Nabsys OhmX Platform delivers the highest resolution for whole-genome SV verification and analysis to support your research. Learn more at nabsys.com/products.

Find additional OhmX Platform Resources at nabsys.com/resources

References

1. Wolf, D. & Rotter, V. Major deletions in the gene encoding the p53 tumor antigen cause lack of p53 expression in HL-60 cells. *Proc. Natl. Acad. Sci.* **82**, 790–794 (1985).
2. Mitsudomi, T. *et al.* p53 gene mutations in non-small-cell lung cancer cell lines and their correlation with the presence of ras mutations and clinical features. *Oncogene* **7**, 171–180 (1992).
3. Rowley, J. D., Golomb, H. M. & Dougherty, C. 15/17 Translocation, a consistent chromosomal change in acute promyelocytic leukaemia. *The Lancet* **309**, 549–550 (1977).
4. Singh, S. *et al.* The cancer-associated, gain-of-function *TP53* variant P152Lp53 activates multiple signaling pathways implicated in tumorigenesis. *J. Biol. Chem.* **294**, 14081–14095 (2019).
5. Hiwase, D. *et al. TP53* mutation in therapy-related myeloid neoplasm defines a distinct molecular subtype. *Blood 141*, 1087–1091 (2023).
6. Lin, D.-L. & Chang, C. p53 Is a mediator for radiation-repressed human TR2 orphan receptor expression in MCF-7 cells, a new pathway from tumor suppressor to member of the steroid receptor superfamily *. *J. Biol. Chem.* **271**, 14649–14652 (1996).
7. Vaughan, C. A. *et al.* p53 mutants induce transcription of NF-κB2 in H1299 cells through CBP and STAT binding on the NF-κB2 promoter and gain of function activity. *Arch. Biochem. Biophys.* **518**, 79–88 (2012).
8. de Thé, H., Chomienne, C., Lanotte, M., Degos, L. & Dejean, A. The t(15;17) translocation of acute promyelocytic leukaemia fuses the retinoic acid receptor a gene to a novel transcribed locus. *Nature* **347**, 558–561 (1990).
9. Kakizuka, A. *et al.* Chromosomal translocation t(15;17) in human acute promyelocytic leukemia fuses *RARa* with a novel putative transcription factor, *PML*. *Cell* **66**, 663–674 (1991).
10. Yoshida, H. *et al.* Accelerated degradation of *PML*-retinoic acid receptor alpha (*PML-RARA*) oncoprotein by all-trans-retinoic acid in acute promyelocytic leukemia: possible role of the proteasome pathway. *Cancer Res.* **56**, 2945–2948 (1996).
11. Bridge, J. A. Advantages and limitations of cytogenetic, molecular cytogenetic, and molecular diagnostic testing in mesenchymal neoplasms. *J. Orthop. Sci.* **13**, 273–282 (2008).
12. He, R. *et al.* Conventional karyotyping and fluorescence *in situ* hybridization: an effective utilization strategy in diagnostic adult acute myeloid leukemia. *Am. J. Clin. Pathol.* **143**, 873–878 (2015).
13. Lu, S. *et al.* Genomic structural variants analysis in leukemia by a novel cytogenetic technique: Optical genome mapping. *Cancer Sci.* **115**, 3543–3551 (2024).
14. Oliver, J. S. *et al.* High-definition electronic genome maps from single molecule data. 139840 Preprint at https://doi.org/10.1101/139840 (2017).